====== **GEODYNAMICS** ======

Geodynamic Settings of the Seafloor Relief Formation in the Madagascar Basin from Data of the 29th Cruise of R/V *Akademik Nikolai Strakhov*

**S. Yu. Sokolov[a],*, K. O. Dobroliubova[a], N. N. Turko[a], E. A. Moroz[a],
A. S. Abramova[a], and A. O. Mazarovich[a]**
Presented by Academician K.E. Degtyarev April 4, 2024

Abstract—The morphology of the seafloor of the Madagascar Basin from Mauritius Island to the Southwest Indian Ridge (SWIR) is represented by a ridge-echeloned relief of the spreading basement. The azimuth of the relief differs by ~90° for the basin north of the SWIR and its wedge-shaped sublatitudinal rift system, separated by an abyssal escarpment. A genetic definition of this seafloor relief shape is given. This shape is formed when the ancient basement breaks up and accretion of the crust orthogonal to the azimuth, which existed before the rupture, begins. The formation of a wedge in the eastern part of the SWIR began about 41 Ma ago and is manifested by higher (±1100 m) amplitudes of relief variations than at the basement before the rupture (±250 m). The change in morphology is also associated with the change in the spreading azimuth of the lithospheric block by about 24° north of the SWIR, which opened up a new space for accretion. The morphology of the relief in the wedge and beyond shows the relationship of its parameters with slowdown in the spreading rate by almost three times when the kinematics of the plates have changed. The high-amplitude ridge-echeloned relief in the ultraslow segment of the SWIR with signs of nontransform displacement is combined with the maxima and minima of Bouguer anomalies. According to the published data, serpentized peridotites and basalts are obtained in the localization of the anomalies. These rocks indicate the presence of detachments with the exposure of ultramafic rocks and minimal magmatic output. Bouguer anomalies along the regional profile perfectly reflect deep density inhomogeneties. For intraplate volcanic edifices, they have a much greater deconsolidation in the upper mantle than near the active interplate boundary of the SWIR. According to the seismic tomography data, the absence of a deep upwelling under the newly formed SWIR segment and the presence of a "cold" gap in the "hot" lenses of the mantle indicates the action of tangential forces in the lithosphere that are not associated with general mantle convection. The formation of the new orthogonal rift system with ultraslow rates is an adaptation to variations in the kinematics parameters of the adjacent lithospheric plates.

Keywords: Southwest Indian Ridge, abyssal escarpment, relief morphology, spreading rate and azimuth, Bouguer anomalies, seismotomographic section, "cold" mantle

DOI: 10.1134/S1028334X2460230X

INTRODUCTION

The geodynamic settings of the oceanic basement formation in ultraslow-rate spreading ridges depend on the plate kinematics and the thermal state of the mantle in the area of a divergent boundary [1]. These parameters have an impact on the thickness of the brittle layer and the type of magmatism. The processes that form the basis of tectonogenesis in the area of mid-ocean ridges and, in particular, the Southwest Indian Ridge (SWIR), determine the morphology of the seafloor relief, which is used to interpret the conditions of crust formation. During the 29th cruise of the R/V *Akademik Nikolai Strakhov* (Geological Institute, Russian Academy of Sciences, 2012–2013), the seafloor relief of the Madagascar Basin between the eastern end of the SWIR to the Rodrigues Triple Junction (RTJ) and Mauritius Island was studied (Fig. 1). Few detailed surveys has been done in the basin, with the exception of work directly along the SWIR. An exception is the survey on board the R/V *Marion Dufresne* (France), which was carried out to the southeast of Mauritius Island and the fault zone of the same

[a] *Geological Institute, Russian Academy of Sciences,
Moscow, 119017 Russia*
*e-mail: sysokolov@yandex.ru
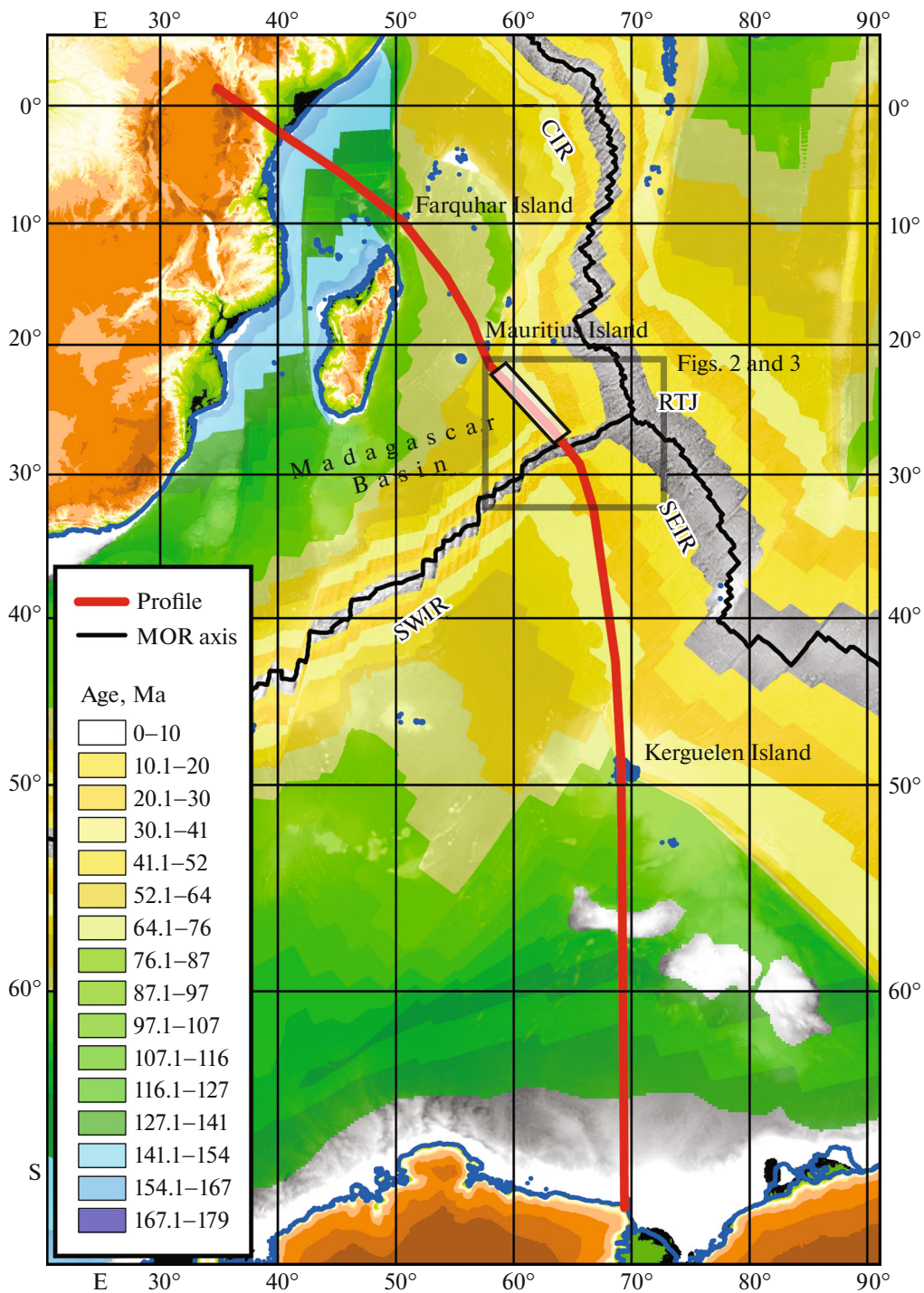
Fig. 1. Position of the regional profile with the seismic tomographic section of Fig. 5-5 and the age of the basement according to [5]. The age interval 0−10 Ma is shown transparent. The relief is shown according to [9] in shades of gray for the oceanic area. A light rectangle shows the position of the Mauritius polygon of the 29th cruise of the R/V *Akademik Nikolai Strakhov* (Geological Institute, Russian Academy of Sciences, 2012−2013). A gray rectangle shows the tablet frames of Figs. 2 and 3. SWIR−Southwest Indian Ridge; SEIR−Southeast Indian Ridge; CIR−Central Indian Ridge; RTJ−Rodriguez Triple Junction.

name, extending along the eastern slope of Mauritius and Reunion islands, but not reaching the SWIR [2]. During the work of the Geological Institute, Russian Academy of Sciences, it was established that the strike

of the ridge-echeloned forms was changed during at least two stages of the evolution of the ridge and its western flank [3]. According to [4], the long-axis segmentation of the SWIR is clearly manifested, reflect-
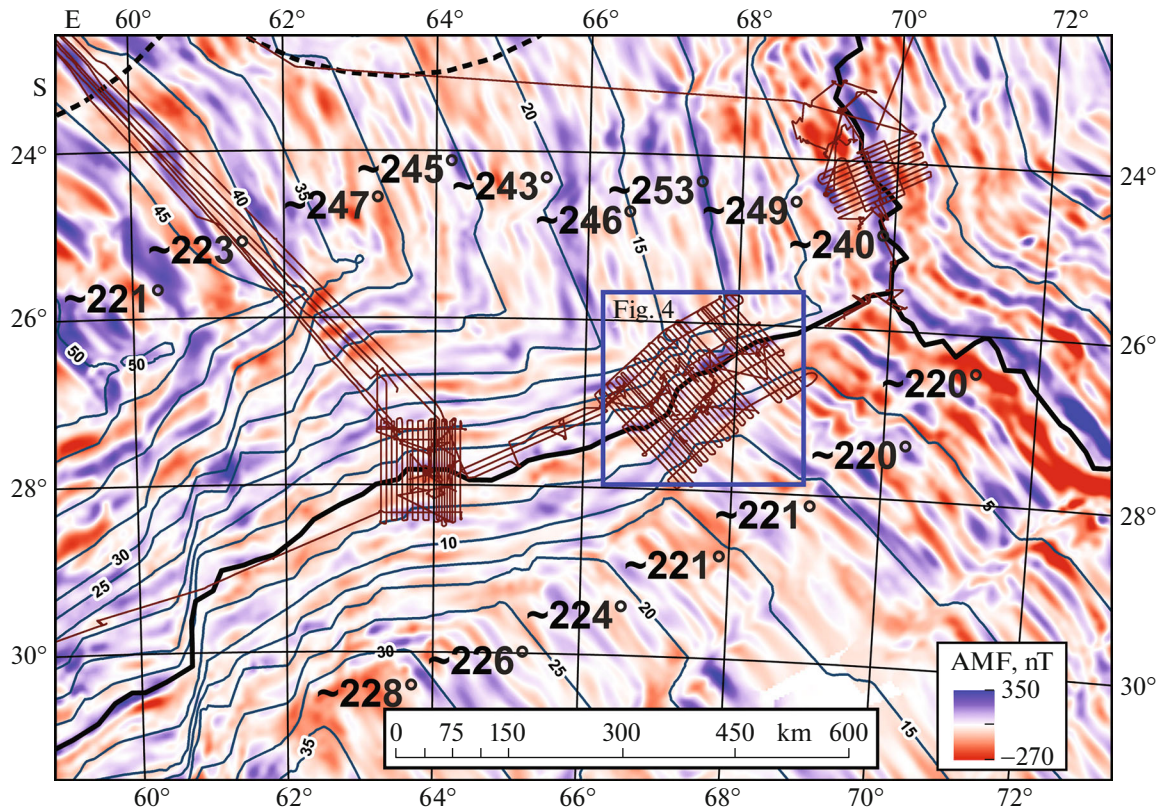
Fig. 2. Anomalous magnetic field (AMF) of the eastern part of the SWIR according to [6]. Isolines with numbers, the age of the basement (million years) according to [5]. Lines: brown, route of the 29th cruise of the R/V *Akademik Nikolai Strakhov* (Geological Institute, Russian Academy of Sciences, 2012−2013); black thickened, ridge axes; black dashed, 200-mile economic zone. The numbers show the values of azimuths of the spreading accretion of the crust in modern coordinates in five-million-year intervals calculated from the age matrix [5]. The blue rectangle shows the position of the tablet in Fig. 4.

ing local restructuring of plate kinematics during the opening of its eastern part. The obtained detailed bathymetric data also allowed us to make an assumption about the contribution of serpentinization processes to the formation of relief macroforms. To achieve a more reliable interpretation of the geodynamics of the area and the seafloor relief, bathymetry should be supplemented with other geophysical data reflecting the deep properties of the crust and mantle, and forming a consistent factual complex. Such data are the seismic tomography, the anomalous gravity field in the Bouguer reduction, and the anomalous magnetic field (AMF). For tomography, their thermal interpretation is the main option for the origin of rate variations. This interpretation is supported by magmatic processes; however, a connection with the material composition and strain sensitivity may still exist. The purpose of this work is to determine and to prove the deep geodynamic factors of variations in the structural pattern of the relief in the study area.

TECTONIC EVOLUTION OF THE AREA

The structure of the SWIR in the east joins the Central Indian Ridge (CIR) in the RTJ area (Fig. 1).

The distribution of the basement ages of the basin, plotted on the basis of data in [5], shows change in the isochron orientation by about 90°. The age of the basement was determined on the basis of the AMF data [6] (Fig. 2) and indexed linear magnetic anomalies. The rupture of submeridional anomalies and the formation of AMF with sublatitudinal orientation for this area have been known for a long time [7]. It follows from the above-mentioned data that, during the time from 43 to 41 Ma, the spreading basement of the western flank of the CIR has been ruptured and a new rift structure of the SWIR was inserted perpendicular to the CIR near the RTJ. We calculated the map of azimuths of spreading directions according to [5]. The azimuths for five-million-year age intervals are designated on the periphery of the sublatitudinal rift system (Fig. 2). It follows from these values that the azimuth of the spreading direction north of the SWIR in modern coordinates changed after the orthogonal rupture of the western flank of the CIR. Before the rupture, the average azimuth was 222°, and after the rupture it was 246°. The jump-like change in the motion vector of the lithospheric plate by about 24° opened a new space along the SWIR rift for the accretion of the
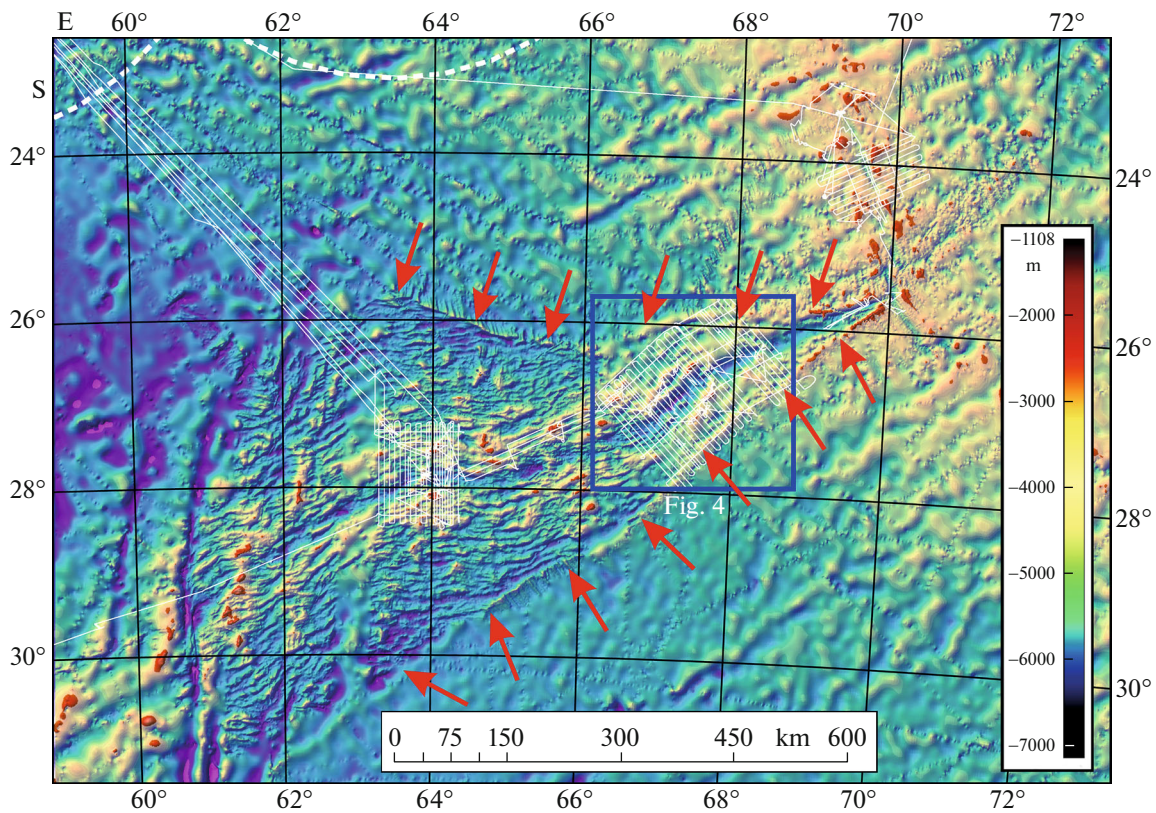
Fig. 3. The seafloor relief of the eastern part of the SWIR according to data [9]. White thin lines, the route of the 29th cruise of the R/V *Akademik Nikolai Strakhov* (Geological Institute, Russian Academy of Sciences, 2012–2013). White dashed line, 200-mile economic zone. The blue rectangle shows the position of the tablet in Fig. 4. Red arrows, abyssal escarpment.

edges of the lithospheric plate split by the spreading basement orthogonal to the initial direction. This space has the shape of a wedge with an apex in the RTJ.

According to [8], the Eocene restructuring of the kinematic parameters of spreading occurred almost in all plates. According to [5], the Africa−Hindustan pair to the north of the SWIR is characterized by a decrease in spreading rates from about 6.3 cm/yr to about 2.1 cm/yr. The change in the spreading azimuth by about 24°, which occurred at the same time (Fig. 2), began to open a window in the wedge-shaped space of the eastern part of the SWIR for the spreading accretion of the crust at a rate of $\sin(24°) \times (2.1 \text{ cm/yr})$, which is about 0.8 cm/yr. Therefore, the eastern part of the SWIR with ultraslow spreading appeared as the form of adaptation to the new rift system due to the rapid (in geological time) change in the kinematics of the lithospheric plate blocks to the west of the CIR. The indicated values of the spreading rates are illustrated by changes in the distances between the isochrones of the basement age (Fig. 2).

Accretion of the magmatic basement with the described change in the plate kinematics is accompanied by the formation of the specific form of relief (*abyssal escarpment*) (Fig. 3), which frames the wedge-

shaped area formed after the change in the motion parameters. Its definition, containing elements of structure and genesis, can be formulated as follows: *An abyssal escarpment is an oceanic intraplate linear form of the seafloor that is a step, hundreds of kilometers long with slope angles greater than 10° and with a depth difference of 1000 to 2000 meters. It is formed during the splitting and tension of the ancient oceanic crust orthogonal to the azimuth of spreading that existed before the splitting, and during the accretion of the crust, also orthogonal to the initial azimuth with the formation of the new ridge-echeloned forms of relief in the deepened base of the escarpment, joining with older relief forms at angles of about 90°.* A detailed example of the abyssal escarpment relief is shown in Fig. 4-1 on the basis of the multibeam bathymetry data. It should be noted that similar forms of relief may occur along the sides of passive parts of transform faults under tension that is not transformed into orthogonal spreading. The tension is generally confirmed by deformations of the sedimentary cover accumulated in the fault trough [12, 13].

RELIEF OF THE EASTERN PART OF SWIR SEAFLOOR

The results of the multibeam bathymetric survey of the seafloor relief of the eastern part of SWIR and the
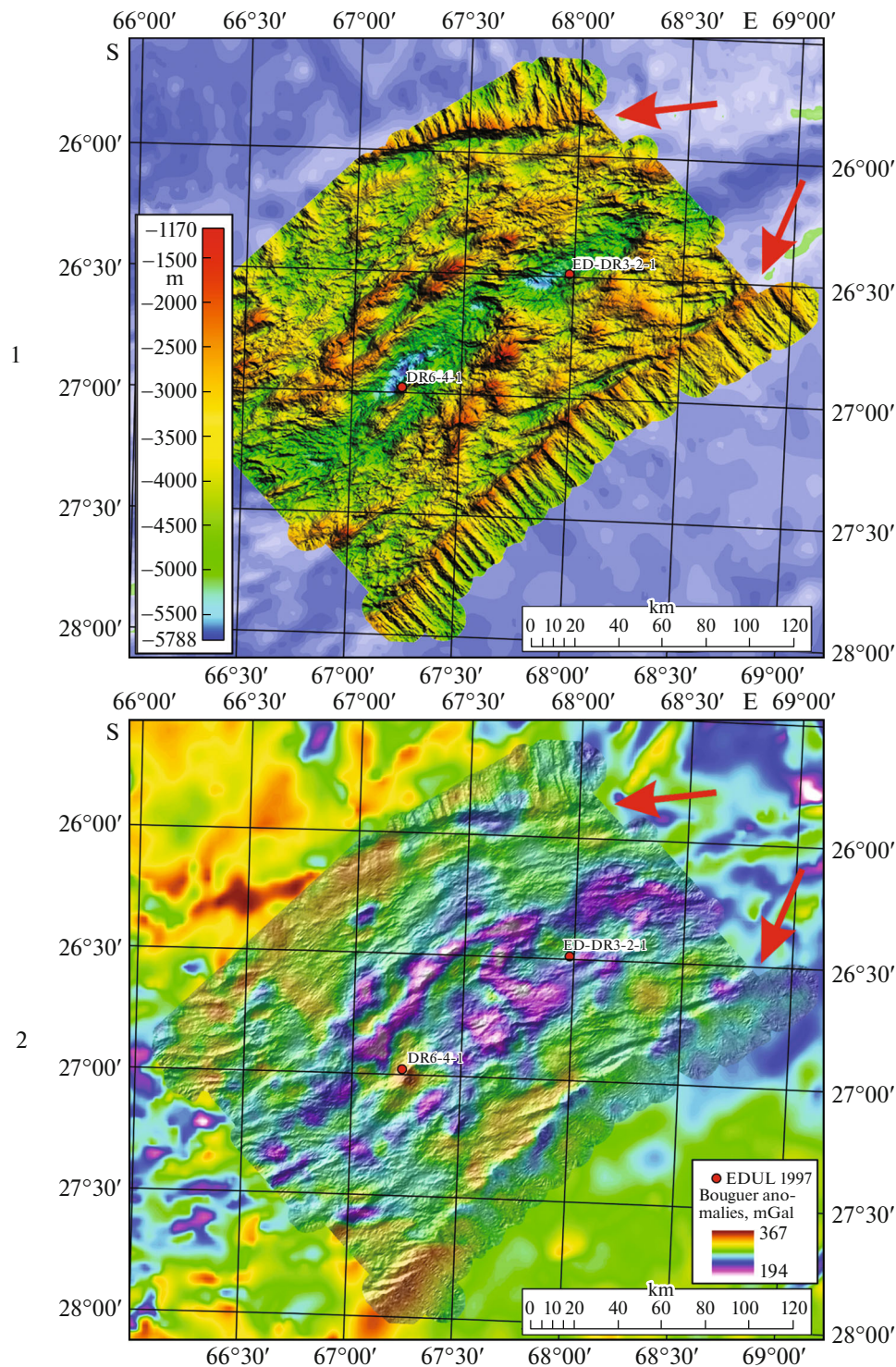
Fig. 4. (1) The seafloor relief and (2) Bouguer anomalies of the eastern part of the SWIR between the abyssal escarrpments (arrows) according to the data of the 29th cruise of the R/V *Akademik Nikolai Strakhov* (Geological Institute, Russian Academy of Sciences, 2012–2013). Position of dredges according to [10, 11]. (1) Shaded relief according to the digital model data on a grid of 100 m, obtained by the SeaBat 7150 multibeam echo sounder; (2) combination of the seafloor relief with Bouguer anomalies. The position of the polygon is shown in Figs. 2 and 3. The arrows show the northern and southern abyssal escarpments.

Madagascar Basin, made during the 29th cruise of the R/V *Akademik Nikolai Strakhov* (Geological Institute, Russian Academy of Sciences, 2012–2013), are shown in Fig. 4-1 and Fig. 5-1, respectively. The digital elevation model (DEM) on a 100-m grid was obtained with the use of the SeaBat 7150 multibeam echo-
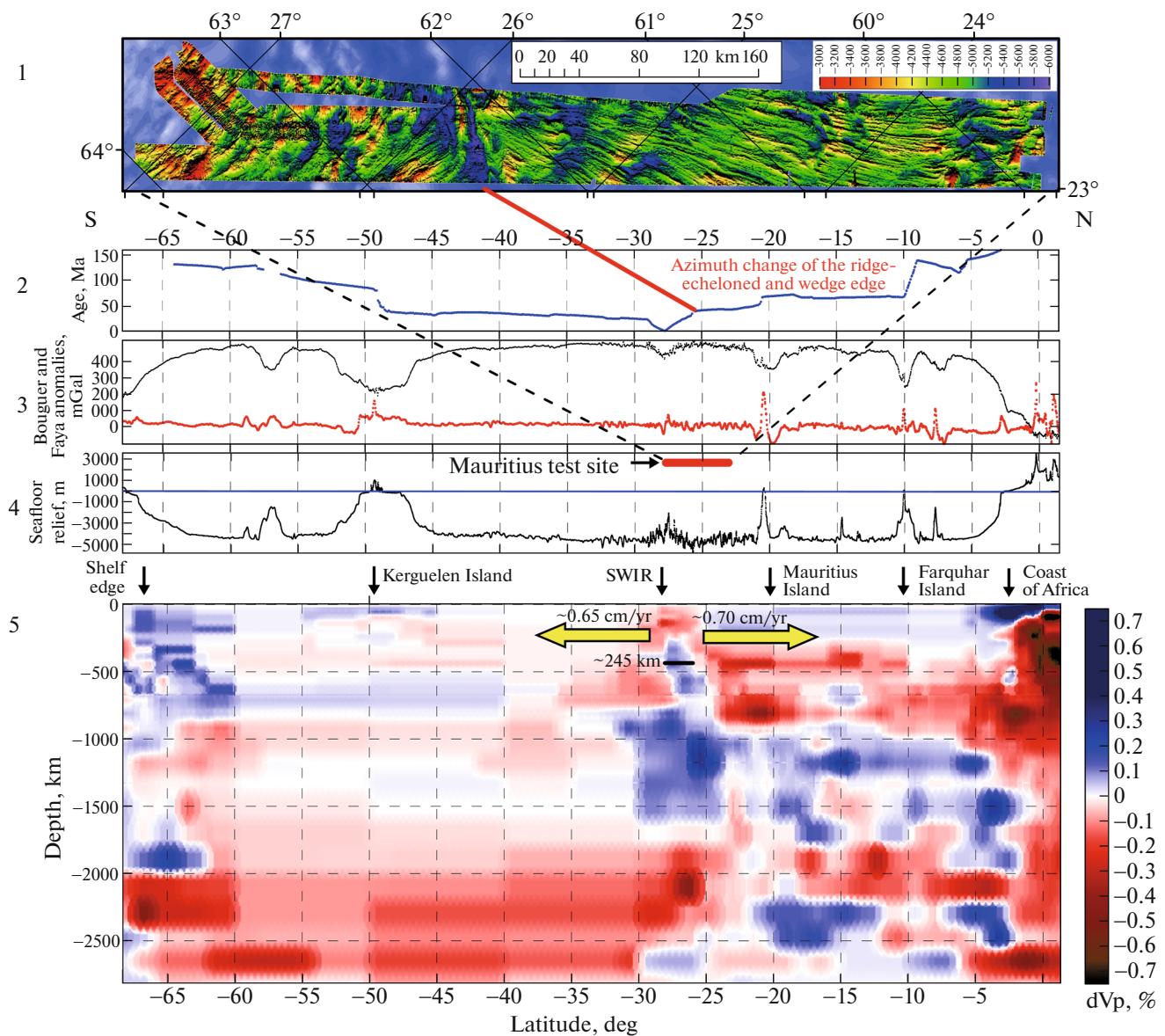
Fig. 5. Correlation of geological and geophysical data along the regional submeridional profile, the position of which is shown in Fig. 1. (1) Shaded relief of the polygon "Mauritius" of the 29th cruise of the R/V *Akademik Nikolai Strakhov* (Geological Institute, Russian Academy of Sciences, 2012−2013) according to the digital model on a grid of 100 m with indication of its position within the profile; (2) profile of the age of the basement according to [5] with indication of the position of the azimuth change of the ridge-echeloned and the edge of the wedge; (3) free air gravity anomalies (Faya) [14] and Bouguer anomalies [15]; (4) seafloor relief [9]; (5) seismic tomographic section of the volumetric model UU-P07 [16], yellow arrows show the direction of the plate drift in projection on the section plane.

sounder (Denmark). For the SWIR (Fig. 4-1), it illustrates the abyssal escarpment defined above. The maximum height of the escarpment is about 1600 m. In the relatively higher parts of the basin floor, bounded by the upper edge of the southern and northern escarpments, the amplitudes of the basement relief, formed at spreading rates of about 2.1 cm/year are ±250 m and are characterized by a regular structural pattern of ridge-echeloned relief. The escarpment walls are modified by vertical ledges, which are consistent with the ridges composing the seafloor of the adjacent abyssal basin. However, the marginal escarpments are distinctly unconformable in azimuth with the spreading structures composing the body of the wedge. Within the limits of the wedge, defined by the ledge geometry, this fact points to the rupture of the single spreading basement and the emplacement of the previously non-existent rift segment orthogonal to the CIR, which was illustrated by the AMF data (Fig. 2).

Spreading in the new rift segment of the wedge proceeds at ultraslow rates of about 0.8 cm/yr. As a result,

the relief that differs from the relief of the basement with higher rates on the uplifted wings of the escarpments is formed (Fig. 4-1). Its ridge structure is characterized by a significantly larger amplitudes of the relief, about ±1100 m. In addition, the maximum height difference within the polygon from the bottom of the rift valley (−5788 m) to the tops of isometric mountains on its sides (−1170 m) is about 4600 m. Such depths of the rift axis indicate accretion of the crust under the conditions of low magmatic output under slow spreading [17]. The increase in amplitude of the seafloor relief with decreased spreading rates is a typical property of oceanic rifting. It was shown experimentally for the geodynamic setting with the slowing-down kinematics of plates with a physical modeling unit of the Earth Science Museum of Moscow State University [18, 19].

The amplitude of the relief reaches its highest value with the SWIR from 67°00′ to 67°45′ E, where the rift axis is bent indicating its nontransform displacement. In this example, this bend is inherited and repeats the general geometry of the northern escarpment (Fig. 3), which in this longitudinal interval has formed at a local deviation of the spreading azimuth up to 253° (Fig. 2). Comparison of the anomalous relief of the indicated interval with Bouguer anomalies (Fig. 4-2) in the semitransparent matching mode shows the presence of a very contrasting values of this reduction from 194 to 367 mGal. The largest scatter in the amplitudes of Bouguer anomalies is observed directly in the zone of nontransform displacement. The field of the maximum of near-axis anomalies was sampled by dredging according to [10, 11]; serpentized peridotites were sampled at the EDUL DR6 station (Fig. 4). This confirms the presence of spreading with a low magmatic output and the exposure of dense upper mantle rocks to the seafloor surface along the detachment planes. At EDUL DR3 station (Fig. 4), basalts were sampled that correspond to a small local minimum of Bouguer anomalies, which is typical for magmatic structures of the oceanic rifts.

The rift interval from 67°00′ to 67°45′ E contains both extensive isometric minima of Bouguer anomalies, which are most likely basaltic fields, and the minima elongated along high-amplitude ridges, which may be strongly serpentinized rocks of the upper mantle. In our opinion, in the absence of dredging data on these ridges, the variant with altered peridotites seems to be more likely. Comparison of the positions of dredging with peridotites according to [20] with Bouguer anomalies is also an arguement in favor of this version. About 70% of the serpentinites, described in this work for the SWIR interval from 62° to 65° E are localized at the maxima of the anomalies, the remaining, about 30%, at the minima that coincide with the high-amplitude ridge-echeloned relief.

RELIEF OF THE MADAGASCAR BASIN SEAFLOOR

The DEM of the Mauritius polygon on a 100-m grid is shown in Fig. 5-1. The polygon is about 60 × 600 km in size and extends from the southern boundary of the 200-mile economic zone of Mauritius Island to the inner part of the SWIR wedge near the isochrone of 15 Ma. At 25°40′ S, the polygon crosses the northern limit of the wedge, where the azimuth of the ridge-echeloned relief changes by about 90° (Fig. 5-1). The similar pattern is observed from the detailed survey data in the eastern part of the SWIR (Fig. 4-1). As was determined from the AMF data (Fig. 2), this area was formed by the rupture of the spreading basement and by the initiated accretion of the oceanic crust at the rupture site along a direction orthogonal to the rupture and manifested in the form of an abyssal escarpment. The Mauritius test site also shows an increase in relief amplitudes at the transition to the ultraslow spreading region inside the wedge-shaped area (Fig. 3) associated with changes in the kinematics parameters of a block of the lithospheric plate to the north of the rupture.

The position of the regional profile (Fig. 1) outside the limits of the wedge mainly run almost along the same-age segments of the basement. The ages along the profile (Fig. 5-2) have segments with constant values, which run along the basement with a sublatitudinal orientation of spreading. The V-shaped change in the ages on both sides of the ridge with a dramatical increase in age over a small segment of space (low spreading rates) can be seen only in the wedge-shaped region of the SWIR adjacent to the RTJ.

Bouguer anomalies (Fig. 5-3) have almost constant values within the same-age sections of the basins, but show deep minima in the areas with zones of deconsolidation in the upper mantle: the SWIR with a drop of ~80 mGal, Kerguelen Island with a drop of 290 mGal, Mauritius Island with a drop of 150 mGal, and Farquhar Island with a drop of 250 mGal. All the active magmatic zones listed are antipodally manifested in the relief (Fig. 5-4).

According to the UU-P07 model (Fig. 5-5), Bouguer anomalies near the intraplate volcanic formations in the seismic tomography section do not have vertical supply channels in the mantle expressed in anomalies of the "plume" type. However, in the depth interval from 100 to 500 km to the south of SWIR and from 300 to 900 km to the north of it, "hot" lenses with signs of horizontal stratification are established. The presence of such lenses at these depths is found mainly in the Indian Ocean. The vertical supply canals approaching the volcanic edifices in the basins, most likely, have widths smaller than the resolution of tomography in this model (about 50 km). Directly beneath the SWIR, at depths up to 1500 km, there is no upwelling "hot" mantle flow; the horizontal "hot" lenses have a gap beneath the SWIR represented by the "cold" mantle

volume. This indicates the absence of the connection of this rift structure with mantle anomalies of the "plume" type. Together with other specific features of the SWIR formation, this indicates the presence of a tangential impact on the horizontal kinematics of the plate and sublithospheric currents formed due to the processes not related to the general mantle convection directly in this rift structure.

The eastern part of the SWIR with a wedge-shaped structure, bounded by escarpments, arose as a zone of the local rupture of the plate with a single tomographic structure of the mantle beneath it and as a result of tension in the process of adapting to the inhomogeneous kinematics of the African, Indo-Australian, and Antarctic plates adjacent to the South Pacific Ocean. An alternative estimate of the spreading rate from the width of the "cold" vertical anomaly of the rates beneath the SWIR structure (Fig. 5-5), equal to about 245 km, gives a value of 0.65−0.7 cm/yr, which is in general agreement with the value obtained from the AMF data. During the formation of the rupture in the eastern part of the SWIR, the ultraslow accretion of the crust began with an orthogonal morphology of the ridge surface of the basaltic basement, different from the morphology of the faster western flank of the CIR.

CONCLUSIONS

(1) The intraplate oceanic form of the seafloor relief, called an *abyssal escarpment*, is primarily defined. The abyssal escarpment is formed during a rupture of the ancient basement at the beginning of accretion of the crust at the spreading azimuth, which is orthogonal to the azimuth existing before the rupture. Such a change in the direction of geodynamic processes of the lithosphere accretion is confirmed by the AMF analysis.

(2) The orthogonal wedging of the SWIR rift into the CIR has formed the ridge-echeloned spreading relief on the surface with the orientation differing from the older one (older than ~41 Ma) by about 90° and by the higher amplitudes (±1100 m). The change in morphology is associated with the rupture of the CIR western flank, when the azimuth of the spreading of the lithospheric block has changed by 24° north of the SWIR. This opened the space for accretion of the crust along the new rift system, which was separated from the old basement by the abyssal escarpments, and formed a wedge-shaped rift segment. The morphology of the relief in the wedge and beyond its boundaries shows that its parameters are related to the slowing down of the spreading rate by a factor of almost three with changes in the global kinematics of the plates.

(3) The high-amplitude ridge-echeloned relief in the ultraslow segment of the SWIR with signs of non-transform displacement coincides with the maxima and minima of Bouguer anomalies. In the area of these anomalies, serpentinized peridotites and basalts were sampled, indicating the presence of detachments with exposure of ultramafic rocks and minimal magmatic output.

(4) Bouguer anomalies along the regional profile fully reflect the deep density heterogeneities, which, for intraplate volcanic edifices, have much greater deconsolidation in the upper mantle than near the active interplate boundary of the SWIR.

(5) The absence of a deep upwelling flow beneath the newly formed segment of the SWIR and the presence of the "cold" rupture in the mantle "hot" lenses indicate the action of tangential forces moving the lithospheric plates and not related to the general mantle convection, but possibly related to the convection in the upper mantle level up to 1000 km. The junction of the eastern part of the SWIR with the CIR about 41 Ma ago formed a new orthogonal rift structure with slower rates, which was the adaptation to variations in the kinematic parameters of the adjacent lithospheric plates.

CONFLICT OF INTEREST

The authors of this work declare that they have no conflicts of interest.

REFERENCES

1. E. P. Dubinin, A. V. Kokhan, and N. M. Sushchevskaya, Geotectonics **47** (3), 131−156 (2013). https://doi.org/10.1134/S0016852113030023

2. J. Dyment, Y. Gallet, et al., InterRidge News **8** (1), 25−31 (1999).

3. N. N. Turko, in *Proc. 22nd Int. Sci. Conf. (School) on Marine Geology "Geology of Seas and Oceans"* (Shirshov Inst. Oceanol. Russ. Acad. Sci., Moscow, 2017), Vol. 5, pp. 249−253 [in Russian].

4. K. O. Dobrolyubova, Vestn. Kamchatskoi Reg. Assots. Uchebn.-Nauchn. Tsentra Nauki Zemle, No. 2 (42), 57−66 (2019). https://doi.org/10.31431/1816-5524-2019-2-42-57-66

5. R. D. Müller, M. Sdrolias, C. Gaina, and W. R. Roest, Geochem., Geophys., Geosyst. G3 **9** (4), 1−19 (2008). https://doi.org/10.1029/2007GC001743

6. S. Maus, U. Barckhausen, H. Berkenbosch, N. Bournas, J. Brozena, V. Childers, F. Dostaler, J. D. Fairhead, C. Finn, R. R. B. von Frese, C. Gaina, S. Golynsky, R. Kucks, H. Luhr, P. Milligan, S. Mogren, R. D. Müller, O. Olesen, M. Pilkington, R. Saltus, B. Schreckenberger, E. Thebault, and F. C. Tontini, Geochem. Geophys. Geosyst. G3 **10** (8), 1−12 (2009). https://doi.org/10.1029/2009GC002471

7. D. Sauter, V. Mendel, C. Rommevaux-Jestin, P. Patriat, and M. Munschy, Mar. Geophys. Res. **19**, 553−567 (1997).

8. C. Gaina and J. Jakob, Tectonophysics **760** (6), 136−151 (2018). https://doi.org/10.1016/j.tecto.2018.08.010

9. GEBCO 15" Bathymetry Grid. Version 2019. http://www.gebco.net.

10. C. M. Meyzen, J. N. Ludden, E. Humler, B. Luais, M. J. Toplis, C. Mével, and M. Storey, Geochem. Geophys. Geosyst. **6**, Q11K11 (2005). https://doi.org/10.1029/2005GC000979

11. M. Seyler, D. Brunelli, M. J. Toplis, and C. Mével, Geochem. Geophys. Geosyst. **12**, Q0AC15 (2011).

12. A. O. Mazarovich, K. O. Dobrolyubova, V. N. Efimov, S. Yu. Sokolov, and N. N. Turko, Dokl. Earth Sci. **379** (6), 615−620 (2001).

13. S. Yu. Sokolov, *Equatorial Part of the Atlantic Ocean: Tectonics and Geodynamics. Sci. Works Geol. Inst. Russ. Acad. Sci.* (Nauchn. mir, Moscow, 2018), Issue 618 [in Russian].

14. D. T. Sandwell and W. H. F. Smith, J. Geophys. Res.: Solid Earth **114** (B1), 1−18 (2009). https://doi.org/10.1029/2008JB006008

15. G. Balmino, N. Vales, S. Bonvalot, and A. Briais, J. Geodesy **86**, 499−520 (2012). https://doi.org/10.1007/s00190-011-0533-4

16. D. G. Van der Meer, D. J. Van Hinsbergen, and W. Spakman, Tectonophysics **723**, 309−448 (2018).

17. S. G. Skolotnev, K. O. Dobrolyubova, A. A. Peyve, S. Yu. Sokolov, N. P. Chamov, and M. Ligi, Geotectonics **56** (1), 1−21 (2022). https://doi.org/10.1134/S0016852122010083

18. A. L. Grokhol'skii, E. P. Dubinin, G. D. Agranov, M. S. Baranovskii, Ya. A. Danilov, P. A. Domanskaya, A. A. Maksimova, A. I. Makushkina, A. O. Rashchupkina, A. I. Tolstova, A. N. Filaretova, Yu. A. Sheptalina, and E. L. Shcherbakova, Zhizn' Zemli **42** (4), 485−501 (2020). https://doi.org/10.29003/m1778.0514-7468.2020_42_4/485-501

19. S. Yu. Sokolov, G. D. Agranov, V. A. Kulikov, A. V. Zayonchek, and A. L. Grokholsky, Dokl. Earth Sci. **514** (1), 29−37 (2024). https://doi.org/10.1134/S1028334X23602213

20. M. Bickert, M. Cannat, A. Tommasi, S. Jammes, and L. Lavier, Geochem., Geophys., Geosyst. **22**, e2020GC009434 (2021). https://doi.org/10.1029/2020GC009434

Translated by V. Krutikova